Lifetimes and branching ratios of excited states in La^-, Os^-, Lu^-, Lr^-, and Pr^-

Steven M. O'Malley and Donald R. Beck
Physics Department, Michigan Technological University, Houghton, Michigan 49931, USA
(Received 21 December 2009; published 5 March 2010)

Relativistic configuration-interaction calculations have been performed for all possible $E1$, $M1$, and $E2$ transitions between bound anion states of La^- and Os^-. We pay particular attention to $E1$ transitions in each case that may be of use in laser cooling of these anions. Although the La^- transition energy is approximately one-third of the Os^- transition, our results indicate that the Einstein A coefficient is nearly two orders of magnitude larger, which would lead to more efficient laser cooling. We have also explored long-lived opposite-parity excited states in Lu^- and Lr^- which are restricted to $M2$ decay by selection rules. Finally, in Pr^-, we find sufficient mixing between a weakly bound excited $4f^25d^26s^2$ state with a nearby $4f^36s^26p$ resonance to result in a lifetime similar to that of the other excited anion states, despite the fact that the dominant configurations of these $M1$ and $E2$ transitions differ by two electrons.

DOI: 10.1103/PhysRevA.81.032503 PACS number(s): 31.15.am, 32.70.Cs, 31.15.vj, 32.10.Hq

I. INTRODUCTION AND MOTIVATION

While Os^- is the only atomic anion with an experimentally observed [1,2] opposite-parity excited state, our relativistic configuration-interaction (RCI) lanthanide and actinide studies [3–5] have predicted many other possible candidates with both even and odd bound anion states, including La^-, Ce^-, Gd^-, Tb^-, Th^-, Pa^-, U^-, and Np^- (opposite-parity excited states are also predicted in Lu^- and Lr^-, but $|\Delta J| = 2$ relative to the anion ground state precludes an $E1$ transition). Observation of these excited states would be difficult due to the fact that the transition energies in these weakly bound systems are on the lower edge or below the photon energy range currently accessible by tunable continuous-wave lasers (most cases are $\sim$0.2 eV or less). The two exceptions are La^- and Ce^- [4], each of which have several potential candidates for $E1$ transitions that lie $>$0.3 eV above the anion ground state. These opposite-parity excited states are also predicted by other computationalists using density-functional theory in the La^- case [6] and multireference configuration-interaction methodology in the Ce^- case [7], and while laser photodetachment electron spectroscopy experiments [8,9] designed to measure electron affinities have not definitively measured these states, it has been suggested that some features in the spectra [4,8–10] correspond to photodetachments from them.

In this RCI excited-state study we have identified a transition in La^- that is perhaps the best candidate among the lanthanide and actinide anions for potential use in laser cooling. We have also used the improved wave functions of our recent studies [4,5] to compute lifetimes of extremely long-lived ($M2$ transition) states in Lu^- and Lr^-. Finally, calculations exploring mixing of two different even configurations in Pr^- have proven fruitful as a verification of the assumption in our recent work [3–5] that states of different $4f$ or $5f$ occupancy can be reasonably treated separately with universal jls restrictions on the f electrons.

II. LASER COOLING IN ATOMIC ANIONS

A. Os^- and La^- as candidates

Laser cooling of atomic anions has been suggested by Kellerbauer and Walz [11] as one step in a process of producing ultracold antihydrogen. At low temperature, Coulomb repulsion between trapped antiprotons and atomic anions would prevent annihilation but allow a transfer of momentum to sympathetically cool the antiprotons (positrons would later be introduced after the anions are removed from the trap). Of course, a similar application of sympathetic cooling could be applied to any atomic or molecular anion or negatively charged particle, employing the efficient laser-cooled species as a buffer.

Os^- was proposed as the anion of choice due to the identification of the weakly bound opposite-parity state by Bilodeau and Haugen [1]. Unpublished preliminary calculations by our own group concurred with the identification of a parity-changing $E1$ transition, but suggested that it would be spin forbidden with dominant LS terms $5d^76s^2\ {}^4F \rightarrow 5d^66s^26p\ {}^6D$. A later measurement by Warring *et al.* [2] improved the precision of the transition frequency by two orders of magnitude and also lowered the Einstein A coefficient from a previous estimate of $\sim 10^4$ s^{-1} [1] to 330 s^{-1} [2] (commensurate with a spin-forbidden $E1$ transition). Members of the same experimental group (Fischer *et al.* [12]) also performed hyperfine measurements that identified the upper state as ${}^6D_{9/2}$ (by observing ten peaks in the spectrum rather than eight [12]). The $\sim$15-meV difference between this bound state, 11.48(12) meV [1], and a low-lying shape resonance, 3.52(12) meV [1], above threshold, make it difficult for RCI calculations to definitively distinguish which of $J = 7/2$ or $J = 9/2$ is lower, since this energy difference is within our expected correlated energy level accuracy of $\sim$30 meV.

Of course, the ideal candidate for laser cooling is a two-level system, and one difficulty of Os^- is the need for repumping of the ${}^4F^e_{7/2} \rightarrow {}^6D^o_{9/2}$ transition [11] indicated in Fig. 1. Also shown in Fig. 1 is our proposed alternate laser-cooling candidate in La^-, a ${}^3F^e_2 \rightarrow {}^3D^o_1$ spin-allowed $E1$ transition whose upper state has three negligible $M1/E2$ decay branches and a weak spin-forbidden $E1$ branch to the excited ${}^1D^e_2$ level. The levels in Fig. 1 are plotted with J increasing to the right; the energies in Os^- are experimental [1] except for $J = 3/2$ and $J = 5/2$, which are revised in this work; and the La^- energies are RCI predictions from our most recent lanthanide study [4].

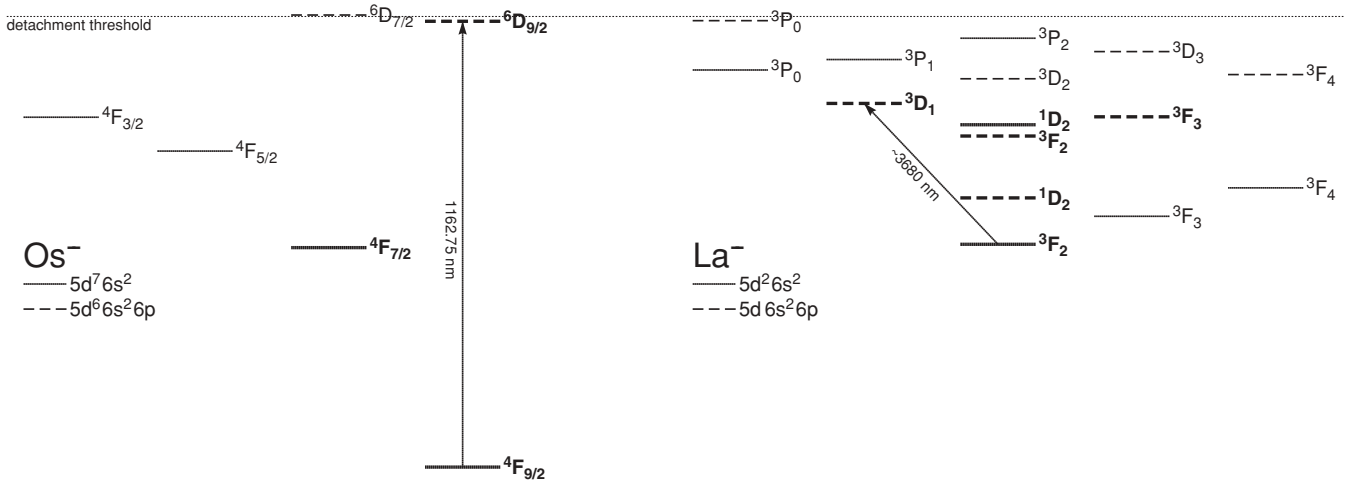

FIG. 1. Bound states of Os^- and La^- plotted with J increasing to the right on the same energy scale: electron affinities of 1.077 80(12) eV [1] for Os^- and 0.545 eV [4] for La^-. Levels of the proposed laser-cooling transitions as well as lower states of possible decay channels from the upper states are shown in bold.

B. Os^- calculations: $5d$ subgroup jls restrictions

In addition to the focus on transition probabilities, these Os^- calculations are ideally suited to testing whether our methodology of applying universal jls restrictions on subgroups of electrons can be usefully applied to transition-metal d^k configurations. In our recent lanthanide and actinide studies [3–5], we developed a procedure of rotating basis functions within the $4f^n$ and $5f^n$ portions of the RCI multielectron bases based on composition of the low-lying neutral attachment thresholds. The portion of the rotated f^n basis with negligible contribution to the RCI wave functions in the levels of interest is discarded, and the limited f^n basis is incorporated into every correlation configuration. This process resulted in minimal energy losses in the bound anion states and neutral thresholds while reducing the basis size in the midrow elements by more than an order of magnitude; for example, in Eu^- (Am^-) the $4f^7$ ($5f^7$) electrons were restricted to $j = 7/2$ only, and the basis was then further rotated to a single function (from 50 possible in $j = 7/2$) composed of a linear combination of the ^8S and ^6P terms. If such a methodology could be applied to d^k subgroups, it might considerably reduce the complexity of transition-metal calculations as well.

Unfortunately, the fact that valence d subshells are not corelike actually precludes such a treatment, principally due to the need to include configurations with differing d occupations. For example, $4f6s$ pair replacements in lanthanide test calculations contribute at most a few tens of meV to correlation energies with negligible difference between multiple anion levels or between anion and neutral calculations. Since this correlation contributes little to mixing between levels or absolute energy difference for binding energy calculations, the RCI bases can be greatly simplified by freezing the $4f$ occupation. In contrast, for transition-metal cases, $5d6s$ pair replacements can contribute half an eV or more (>1 eV for $5d6s \rightarrow pf$ in the even Os^- levels).

We have nevertheless applied the jls restriction technique individually to each $5d^k$ occupation. Ironically, the potential usefulness of the method is *a priori* limited due to the lesser complexity of the d^k configurations, for example, a maximum of 10 basis functions for $j = 5/2$ in the half-filled d^5 subshell versus the aforementioned 50 functions for f^7 $j = 7/2$. In the case of Os^- we also found that the jls composition within the d^k electrons changed for each anion or neutral level in contrast to the lanthanide and actinide calculations, where careful analysis led to f^n bases that were simultaneously optimized to all states for each anion regardless of total J.

This problem is due partly to the fact that different types of correlation configurations were optimized by different ls terms. To recognize these different patterns, one must prepare data such that the composition within the basis functions of a particular d^k subgroup with a particular j can be separately tracked when combined with each basis function of the remainder of the configuration. For example, for even Os^- $5d^76s^2$ levels, the $5d^6$ subgroup of some correlation configurations can potentially range from $j = 0$ to $j = 6$, depending on the maximum j of the remaining three-electron group (nine total) and the total J of the anion. For each of those $5d^6$ j's we found up to five recurring patterns in the ls composition within that j that would add non-negligible correlation to the $5d^76s^2$ level: one for each of the three single electron $5d$ replacements to vs, $vd_{3/2}$, and $vd_{5/2}$, as well as one for double replacements from either $5d_{3/2}6s$ or $5d_{5/2}6s$ (vl denotes an RCI screened hydrogenic "virtual" orbital). Not all of these five possible rotations are always present; for example, $(5d^6)_{j=2}6s^2vs$ is only present in the Os^- $J = 3/2$ and $J = 5/2$ calculations. Nevertheless, the number of basis functions for each j of $5d^6$ only ranges from one to eight, and even though one can occasionally retain just two or three out of seven or eight basis functions, we were only able to reduce each RCI basis (including other $5d^k$ occupancies with $k > 5$) by ~40%–50% while retaining acceptable correlation energy losses of a few meV. While this result is discouraging with regard to application to transition metals, it underscores the power of the jls universal restrictions on the lanthanide and actinide corelike f electrons to which the method is ideally suited.

C. Energies, *LS* composition, and Einstein *A* coefficients

Ultimately, we have abandoned the *jls* restriction idea here for an older and simpler winnowing process. That is, we simply remove basis functions from each stage of the Os^- calculations that have both RCI coefficients and correlation energies below a preselected threshold, creating more space within our coded 20 000 RCI basis limit for subsequent correlation, for example, additional or higher-l virtual orbitals and second-order effects. While simple enough in practice, this method is rarely useful for systems with more than a few levels of interest per J-parity calculation, since one often finds a sizable fraction of basis functions that are small for each level but very few that are small for all of them. In the case of Os−, we are only concerned with one level per J for either parity, and higher unbound levels of each J are over 1 eV above the levels of interest with negligible mixing with the lower states. In contrast to the *jls* restrictions, we were able to reduce the RCI bases by approximately a factor of three with only a few *tenths* of an meV loss in energy. This approach greatly speeds up the calculations as well, since retaining *jj* parents within the $5d^k$ subgroups allows for many more zero elements in our relativistic two-particle Hamiltonian matrix; that is, in addition to the remainder of the nine-electron Os^- configurations, $5d_{3/2}$ and $5d_{5/2}$ occupations can also determine whether two basis functions differ by more than two electrons (rotated bases retain linear combinations of all the $5d^k jj$ functions).

RCI energies and *LS* composition for the Os^- states are shown in Table I, where we use the experimental energy [1] of the lowest level of each parity as a reference point (a similar table of our La^- RCI data is available elsewhere [4]). By doing so, we can place the anion states relative to one another rather than neutral thresholds, eliminating the need to open the shallow core as was done in the earlier study by our group [13] (core-valence correlation is assumed to have a negligible differential contribution to anion states of the same configuration compared to anion-neutral differences). This leaves us more room in the RCI basis for second-order effects, which has resulted in the modest reduction in energy differences between the even levels as seen in Table I (these new $J = 3/2$ and $J = 5/2$ values are plotted in Fig. 1).

The inclusion of many second-order effects, triple and quadruple replacements relative to the dominant configuration, introduces other complications, however. A common difficulty with transition-metal calculations is choosing where to stop opening the d subshell. For example, for $Os^- 5d^7 6s^2$ simple first-order calculations including some $5d6s$ pair replacements will contain important correlation configurations such as $5d^7 6p^2$ and $5d^6 6s 6p^2$. Adding $5d6p$ pair replacements to $5d^7 6p^2$ to include similar correlation to this configuration results in unproblematic triple replacements with respect to $5d^7 6s^2$; however, the single $5d \rightarrow 6s$ or double $5d6p \rightarrow 6svp$ replacements added to $5d^6 6s 6p^2$ result in configurations that are effectively $5d^2 \rightarrow 6p^2 + 6pvp$ with respect to $5d^7 6s^2$.

In an attempt to provide appropriate correlation of a few tenths of an eV to the important first-order contributor to lower it with respect to the level of interest, one can do the exact opposite by including several eV of $5d^2$ pair correlation to the zeroth-order configuration. Often, one can mitigate this problem by careful j restrictions on electron subgroups (e.g., $5d6s^2$ triple replacements restricted to $j = 3/2$ and $j = 5/2$), but this usually results in incomplete application of the second-order triple or quadruple replacement. For these calculations, we have removed $5d^2$ correlation from all configurations by zeroing off matrix elements between configurations whose $5d^k$ occupancies differ by more than one, which allows us to stop at $k = 5$ in these calculations; for example, $5d6s$ correlation is added to $5d^6 6s 6p^2$, but $5d^2$ ($k = 4$) is not. A similar process has been used recently [14] to omit interaction between large blocks of basis functions from different second-order configurations with little effect on energies but significant savings in computation time.

This option is important in Os^-, since inclusion of extensive second-order effects in the even calculations led to overcorrelation of $5d^8 6s$, particularly for $J = 3/2$ and $J = 5/2$ which can also include $5d^9$; in one case $5d^8 6s$ was mixing in the $J = 3/2$ level by ∼39% and it was artificially lowered below the $J = 7/2$ level (see Fig. 1). Similar issues also arose in the odd calculations where $5d^2$ correlation was omitted from $5d^6 6s^2 6p$, but $5d6s$ replacements led to overcorrelation ($k = 5$) of $5d^7 6s 6p$ and mixing of this configuration of ∼31%, much greater than that seen in either preliminary calculations that include extensive first-order type j restrictions or our final calculations that have carefully removed this $5d^2$ correlation while relaxing j restrictions and including

TABLE I. RCI binding energies (meV, relative to lowest state of each parity) and *LS* composition (%) of Os^- states. Total J and parity are given in the leading term of each state, and contributions are presented rounded to the nearest percent. The older RCI values [13] have been shifted by 30 meV to match the experimental [1] electron affinity and illustrate the moderate increase in binding of the excited even states in this work.

LS composition	RCI	Old RCI [13]	Expt. [1]
$^6D^o_{7/2}$ 56, ^6P 19, ^4D 15, ^4F 5, ^6F 4, ^2F 1	−17		−3.52(12)
$^6D^o_{9/2}$ 80, ^6F 9, ^4F 9, ^4G 1, ^2G 1	11		11.48(12)
$^4F^e_{3/2}$ 57, ^2D 19, ^2P 18, ^4P 6	279	241	
$^4F^e_{5/2}$ 85, ^2D 12, ^4P 2, ^2F1	341	322	
$^4F^e_{7/2}$ 98, ^2G 2	544	538	553(3)
$^4F^e_{9/2}$ 91, ^2G 9	1078	1078	1077.80(12)

TABLE II. Lifetimes and decay branches of bound excited even ($5d^7 6s^2$) and odd ($5d^6 6s^2 6p$) states of Os^-. Both $^6D^o$ levels have been treated here as the weakly bound $6p$ attachment to the Os^- ground state in order to make the comparison with the experimental transition probability [2]. Energy differences (meV) are determined from experimental values [1] except for the $^4F^e_{3/2,5/2}$ cases, which are taken from these calculations. The exponents in the Einstein A coefficients (s^{-1}) are abbreviated; that is, $1.2[-3] \equiv 1.2 \times 10^{-3}$. The bold entries represent the upper state of the proposed [11] laser-cooling transition and its two possible $E1$ decay channels (see Fig. 1).

Level (τ) Branch (ΔE)	RCI Einstein A coefficient			
	$E1$	$M1$	$E2$	Other $M1/E1$
$^4F^e_{3/2}$ 230 s				
$\rightarrow {}^4F^e_{5/2}$ 62		4.4[−3]	1.2[−8]	6.3[−3] [13]
$\rightarrow {}^4F^e_{7/2}$ 274			6.0[−7]	
$^4F^e_{5/2}$ 4.2 s				
$\rightarrow {}^4F^e_{7/2}$ 212		2.4[−1]	4.4[−7]	1.7[−1] [13]
$\rightarrow {}^4F^e_{9/2}$ 737			4.8[−4]	
$^4F^e_{7/2}$ 420 ms				
$\rightarrow {}^4F^e_{9/2}$ 525		2.4[+0]	6.4[−5]	2.2[+0] [13]
$^6D^o_{7/2}$ 340 μs				
$\rightarrow {}^4F^e_{5/2}$ 330	2.2[+1]			
$\rightarrow {}^4F^e_{7/2}$ 542	6.4[+2]			
$\rightarrow {}^4F^e_{9/2}$ 1067	2.3[+3]			
$^6D^o_{9/2}$ 3.8 ms				
$\rightarrow {}^4F^e_{7/2}$ 542	**3.1[+1]**			
$\rightarrow {}^4F^e_{9/2}$ 1067	**2.3[+2]**			**3.3[+2]** [2]

second-order correlation (in both cases the $5d^7 6s6p$ mixing is ∼3%). Of course, the omitted $5d^2$ correlation is larger for higher k configurations, but the few-tenths-to-half-an-eV differences are determined in smaller auxiliary calculations and reintroduced in the final calculations in the form of shifts in the different blocks' diagonal matrix elements.

Einstein A coefficients for Os^- and La^- are presented in Tables II and III, respectively. We report the length gauge only throughout this work, since cancellation in reduced matrix elements in weak transitions makes accurate velocity gauge calculations notoriously difficult. Also note that all the lifetime tables presented here are ordered by J (low to high) and energy within that J (most bound to least), and the decay channels for each state are similarly ordered. Although, our RCI calculations do place the odd $J = 9/2$ level below the $J = 7/2$ resonance in agreement with the experimental hyperfine measurement [12], the difference is nearly double the 15- meV [1] experimental splitting. As a separate verification, we treated both $J = 9/2$ and $J = 7/2$ as the weakly bound level and calculated transition probabilities for both of them. A preliminary first-order calculation for the $^4F^e_{9/2} \rightarrow {}^6D^o_{9/2}$ $E1$ transition gave a value for A of 320 s^{-1}, fortuitously close to the latest experimental value of 330 s^{-1} [2], while adjustments in RCI bases approaching the final calculations ranged from 480 to 210 s^{-1}, with the final value of 230 s^{-1} resulting from the diagonal shifts described previously. For all these stages, the corresponding $^4F^e_{9/2} \rightarrow {}^6D^o_{7/2}$ transition probability remains approximately an order of magnitude larger than the experimental measurement [2], providing an independent verification that $^4F^e_{9/2}$ is the weakly bound level (cf. LS composition in Table I, which shows greater sextet purity in $J = 9/2$, making this transition more purely spin-forbidden).

With regard to the appropriateness of these two systems as laser-cooling candidates, we note that the La^- transition energy is about a third of the Os^- transition, although when considering momentum transfer per photon and its impact on anion velocity, this difference is somewhat mitigated due to Os^- being ∼37% heavier than La^-. On the other hand, the calculated La^- spin-allowed transition probability is ∼88 times greater than the experimental Os^- value [2], which would lead to a much higher absorption rate. Also, throughout the stages of our RCI calculations, the branching ratio of the Os^- decay to the excited $J = 7/2$ even level remains in the range of 8%–12%, confirming the definite need to repump this transition [11], while our calculations indicate that the proposed La^- upper state decays back to the ground state in >99.98% of emissions, making it a much better approximation of a simple two-level system.

III. LONG-LIVED ($M2$) EXCITED STATES

Plots of our predicted Lu^- and Lr^- states are presented in Fig. 2, and detailed compositions and binding energies are presented elsewhere [4,5]. The interesting situation in both cases is that, when considering single photon transitions up to the octupole moments, there is a state that can only decay by the $M2$ operator; $M1$, $E2$, and $M3$ are precluded by the parity change, $E1$ by $|\Delta J| > 1$, and $E3$ by its strict $J = 0 \not\leftrightarrow J = 2$

TABLE III. Lifetimes and decay branches of bound excited even ($5d^2 6s^2$) and odd ($5d6s^2 6p$) states of La^-. Energy differences (meV) are from the most recent lanthanide RCI electron-affinity study [4], and the exponents in the Einstein A coefficients (s^{-1}) are abbreviated; that is, $1.2[-3] \equiv 1.2 \times 10^{-3}$. The bold entries represent the upper state of the proposed laser-cooling transition and its five possible decay channels (see Fig. 1).

Level (τ) Branch (ΔE)	Einstein A coefficient $E1$	$M1$	$E2$	Level (τ) Branch (ΔE)	Einstein A coefficient $E1$	$M1$	$E2$	Level (τ) Branch (ΔE)	Einstein A coefficient $E1$	$M1$	$E2$
$^3P_0^e$ 5.6 ms				$^3F_2^o$ 1.3 ms				$^3F_3^e$ 260 s			
$\rightarrow {}^3D_1^o$ 80	1.8[+2]			$\rightarrow {}^3F_2^e$ 259	5.3[+2]			$\rightarrow {}^3F_2^e$ 67		3.9[−3]	7.7[−9]
$\rightarrow {}^3F_2^e$ 417			4.6[−4]	$\rightarrow {}^1D_2^o$ 148		4.5[−3]	8.6[−6]				
$\rightarrow {}^1D_2^e$ 131			2.2[−7]	$\rightarrow {}^3F_3^e$ 192	2.6[+2]			$^3F_3^o$ 910 μs			
								$\rightarrow {}^3F_2^e$ 305	1.6[+2]		
$^3P_0^o$ 590 μs				$^1D_2^e$ 3.0 ms				$\rightarrow {}^1D_2^o$ 194		1.7[−2]	4.1[−5]
$\rightarrow {}^3D_1^o$ 198		5.0[−5]		$\rightarrow {}^3F_2^e$ 286		8.8[−3]	4.7[−6]	$\rightarrow {}^3F_2^o$ 46		1.1[−3]	1.0[−8]
$\rightarrow {}^3P_1^e$ 93	1.7[+3]			$\rightarrow {}^1D_2^o$ 175	3.3[+2]			$\rightarrow {}^1D_2^e$ 19	8.8[−3]		
$\rightarrow {}^1D_2^o$ 424			1.6[−3]	$\rightarrow {}^3F_2^o$ 27	9.5[−1]			$\rightarrow {}^3F_3^e$ 238	9.0[+2]		
$\rightarrow {}^3F_2^o$ 276			1.4[−3]	$\rightarrow {}^3F_3^e$ 219		5.5[−3]	6.5[−7]	$\rightarrow {}^3F_4^e$ 170	4.3[+1]		
$\rightarrow {}^3D_2^o$ 139			1.0[−5]	$\rightarrow {}^3F_4^e$ 151			8.6[−7]				
								$^3D_3^o$ 30 μs			
$^3D_1^o$ 34 μs				$^3D_2^o$ 34 μs				$\rightarrow {}^3D_1^o$ 124			1.7[−6]
$\rightarrow {}^3F_2^e$ 337	**2.9[+4]**			$\rightarrow {}^3D_1^o$ 59		2.6[−3]	3.7[−5]	$\rightarrow {}^3F_2^e$ 461	2.1[+1]		
$\rightarrow {}^1D_2^o$ 226		**2.1[−3]**	**3.7[−5]**	$\rightarrow {}^3F_2^e$ 396	3.6[+3]			$\rightarrow {}^1D_2^o$ 350		2.7[−3]	2.9[−4]
$\rightarrow {}^3F_2^o$ 78		**1.4[−6]**	**2.4[−6]**	$\rightarrow {}^1D_2^o$ 285		1.0[−3]	2.2[−4]	$\rightarrow {}^3F_2^o$ 202		8.9[−4]	1.3[−5]
$\rightarrow {}^1D_2^e$ 51	**3.7[+0]**			$\rightarrow {}^3F_2^o$ 137		2.2[−5]	2.9[−5]	$\rightarrow {}^1D_2^e$ 175	4.3[+2]		
$\rightarrow {}^3F_3^o$ 32			**1.2[−8]**	$\rightarrow {}^1D_2^e$ 110	5.4[+0]			$\rightarrow {}^3D_2^o$ 65		2.5[−3]	3.9[−7]
				$\rightarrow {}^3F_3^e$ 329	2.6[+4]			$\rightarrow {}^3F_3^e$ 394	1.8[+3]		
$^3P_1^e$ 2.3 ms				$\rightarrow {}^3F_3^o$ 91		1.3[−5]	4.3[−6]	$\rightarrow {}^3F_3^o$ 156		3.0[−4]	3.6[−5]
$\rightarrow {}^3P_0^e$ 25		1.4[−4]						$\rightarrow {}^3F_4^e$ 326	3.1[+4]		
$\rightarrow {}^3D_1^o$ 105	3.2[+2]			$^3P_2^e$ 1.5 ms				$\rightarrow {}^3F_4^o$ 55		1.2[−5]	7.0[−7]
$\rightarrow {}^3F_2^e$ 442		2.5[−4]	5.4[−4]	$\rightarrow {}^3P_0^e$ 76			4.3[−8]				
$\rightarrow {}^1D_2^o$ 331	7.1[+1]			$\rightarrow {}^3D_1^o$ 156	6.0[+1]			$^3F_4^e$ 300 s			
$\rightarrow {}^3F_2^o$ 183	4.6[−3]			$\rightarrow {}^3P_1^e$ 51		8.8[−4]	1.6[−8]	$\rightarrow {}^3F_2^e$ 135			2.3[−10]
$\rightarrow {}^1D_2^e$ 156		1.8[−3]	9.1[−7]	$\rightarrow {}^3F_2^e$ 493		1.3[−6]	1.8[−4]	$\rightarrow {}^3F_3^e$ 68		3.3[−3]	4.9[−9]
$\rightarrow {}^3D_2^o$ 46	4.5[+1]			$\rightarrow {}^1D_2^o$ 382	4.1[+2]						
$\rightarrow {}^3F_3^e$ 375			3.6[−4]	$\rightarrow {}^3F_2^o$ 234	1.4[+1]			$^3F_4^o$ 540 μs			
				$\rightarrow {}^1D_2^e$ 207		1.2[−2]	2.2[−5]	$\rightarrow {}^1D_2^o$ 295			3.3[−6]
$^1D_2^o$ 30 ms				$\rightarrow {}^3D_2^o$ 97	1.5[+2]			$\rightarrow {}^3F_2^o$147			1.4[−6]
$\rightarrow {}^3F_2^e$ 111	3.2[+1]			$\rightarrow {}^3F_3^e$ 426		1.0[−3]	3.8[−4]	$\rightarrow {}^3D_2^o$ 10			3.4[−11]
$\rightarrow {}^3F_3^e$ 44	1.1[+0]			$\rightarrow {}^3F_3^o$ 188	2.3[+1]			$\rightarrow {}^3F_3^e$ 339	1.5[+2]		
				$\rightarrow {}^3D_3^o$ 32	1.7[+1]			$\rightarrow {}^3F_3^o$ 101		1.1[−2]	2.1[−6]
				$\rightarrow {}^3F_4^e$ 358			4.3[−4]	$\rightarrow {}^3F_4^e$ 271	1.7[+3]		

selection rule. The result is the extremely long lifetimes of these states as presented in Tables IV and V, such that other decay processes (such as collisions in a magnetic trap) are likely to limit the lifetime in a real experimental situation. The two-orders-of-magnitude difference in these lifetimes is primarily attributed to the fact that the ground-state transition in Lu^- is spin forbidden with respect to the dominant terms [4] (the alternate $J = 2$ channel is limited by the small ΔE).

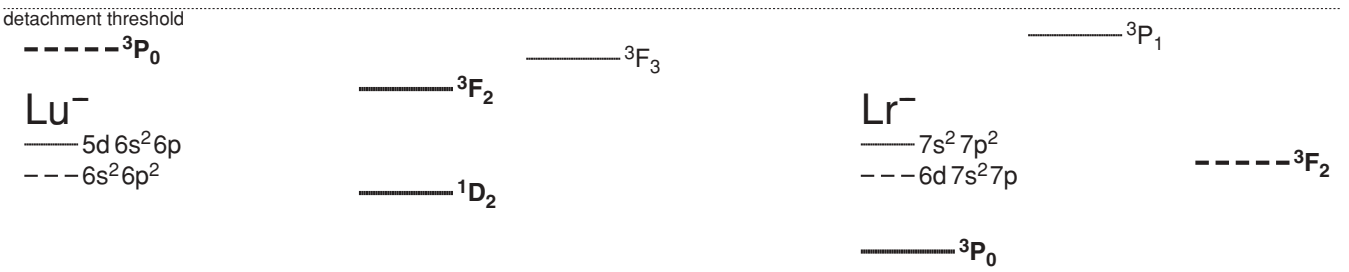

FIG. 2. Bound states of Lu^- and Lr^- plotted with J increasing to the right on the same energy scale: predicted RCI electron affinities of 0.353 eV [4] for Lu^- and 0.465 eV [5] for Lr^-. Levels of the long-lived $M2$ decay channels are shown in bold.

TABLE IV. Lifetimes and decay branches of bound excited odd ($5d6s^26p$) and even ($6s^26p^2$) states of Lu^-. Energy differences (meV) are from the most recent lanthanide RCI electron-affinity study [4], and the exponents in the Einstein A coefficients (s^{-1}) are abbreviated; that is, $1.2[-3] \equiv 1.2 \times 10^{-3}$. The bold entries represent the long-lived state and its two possible $|\Delta J| = 2$ decay channels (see Fig. 2).

Level (τ) Branch (ΔE)	RCI Einstein A coefficient		
	$M1$	$E2$	$M2$
$^3P_o^e$ 2200 *y*			
$\rightarrow {}^1D_2^o$ 275			**1.4[−11]**
$\rightarrow {}^3F_2^o$ 76			**1.8[−13]**
$^3F_2^o$ 58 s			
$\rightarrow {}^1D_2^o$ 199	1.7[−2]	1.0[−4]	
$^3F_3^o$ 14 s			
$\rightarrow {}^1D_2^o$ 257	6.9[−2]	2.6[−4]	
$\rightarrow {}^3F_2^o$ 58	1.8[−3]	5.6[−8]	

With no intermediate J level in Lu^-, it would likely be difficult to observe the odd state unless it is populated in the anion production process itself. In Lr^-, however, a possible weakly bound $J = 1$ level provides a two-step process to populate the $J = 2$ odd state by pumping the $^3P_0^e \rightarrow {}^3P_1^e$ $M1$ transition (~3000 nm) followed by $E1$ decay to $^3F_2^o$ (99.95%). This binding of this $J = 1$ level was increased in our RCI prediction by about 15 meV over earlier Lr^- relativistic Fock-space coupled-cluster calculations [15], despite the fact that our electron affinity was also increased relative to this earlier work by approximately ten times that amount. The most recent intermediate Hamiltonian coupled-cluster calculations [16] prior to our RCI value actually had an electron affinity 11 meV larger than ours but only reported the $^3P_0^e$ and $^3F_2^o$ bound Lr^- states.

Photodetachment from the Lr^- $7s^27p_{1/2}^2$ $J = 0$ [5] ground state should produce a single peak ($7p_{1/2} \rightarrow \epsilon s + \epsilon d_{3/2}$) in a photoelectron kinetic-energy spectrum for incident photon energies above 0.465 eV (our RCI electron affinity) and below ~3.0 eV: the channel to the Lr $6s^26p_{3/2}$ excited state (~1 eV above the $6s^26p_{1/2}$ ground state [15–18]) should be weak due to only 4% mixing of $6s^26p_{3/2}^2$ in the Lr^- ground state [5], and the $6s \rightarrow \epsilon p_{1/2}$ channel is possible above this energy range [16,17]. If the long-lived $6d_{3/2}7s^27p_{1/2}$ state (98% pure [5]) were populated, however, the shift in the peak would be minimal according to our predictions, that is, ΔE of 0.469 eV for the $7p_{1/2} \rightarrow \epsilon s + \epsilon d_{3/2}$ detachment to $6d_{3/2}7s^2$. This state might only be identified by the appearance of a much smaller peak due to $6d_{3/2} \rightarrow \epsilon p + \epsilon f_{5/2}$ detachment to the Lr ground state with ΔE of 0.295 eV (or perhaps more likely only by the emitted 0.214-eV photon from the $^3P_1^e \rightarrow {}^3F_2^o$ spin-forbidden $E1$ decay while populating the state).

TABLE V. Lifetimes and decay branches of bound excited even ($7s^27p^2$) and odd ($6d7s^27p$) states of Lr^-. Energy differences (meV) are from the most recent actinide RCI electron-affinity study [5], and the exponents in the Einstein A coefficients (s^{-1}) are abbreviated; that is, $1.2[-3] \equiv 1.2 \times 10^{-3}$. Note that the strict $J = 0 \not\rightarrow J = 1$ selection rule precludes an $E2$ transition between the two even levels. The bold entries represent the long-lived state and its $|\Delta J| = 2$ decay channel to the Lr^- ground state (see Fig. 2).

Level (τ) Branch (ΔE)	RCI Einstein A		
	$E1$	$M1$	$M2$
$^3P_1^e$ 41 ms			
$\rightarrow {}^3P_0^e$ 414		1.1[−1]	
$\rightarrow {}^3F_2^o$ 244	2.4[+1]		1.1[−10]
$^3F_2^o$ 24 *y*			
$\rightarrow {}^3P_0^e$ 170			**1.3[−9]**

IV. A TEST OF $4f^n$-$4f^{n-1}$ MIXING

Pr^- is an interesting case (plotted in Fig. 3), since unlike the other anions discussed in Sec. I, the second type of bound attachment is of the same parity as the anion ground state (the actinide Pa^- is actually predicted to have both same- and opposite-parity alternate attachments [5]). We have included this case here to test the validity of our assumption that the position of these levels with differing $4f$ occupancies are not much affected by treating them individually in segregated RCI calculations. The binding energy predictions of the six $6p$ attachments to the $4f^36s^2$ $J = 9/2$ neutral ground state [3] were calculated separately from the $6s$ attachment to an excited $4f^25d^26s$ threshold [4]. However, because the two configurations differ by two electrons, $4f^36s^26p$ and $4f^25d^26s^2$, they must be allowed some mixing to produce the $M1$ and $E2$ transition probabilities.

Though we are dealing with a lanthanide near the end of the row, these calculations are nontrivial, because $4f$ one-electron radial wave functions optimized to configurations with differing occupancies for this subshell can be quite different. In fact, initial errors in neutral Nd excited-threshold placement were on the order of 1 eV in an earlier RCI photodetachment study [19]. In these Pr^- calculations, we have used the $4f^3$ optimized radial functions and compensated for the lack of more diffuse functions in the $4f^2$ configurations by including extensive $4f \rightarrow vf$ single replacements. Our final *ab initio* $J = 6$ mixed-configuration calculation places the $4f^25d^26s^25L_6$ level 68 meV above $4f^36s^26p^3K_6$, in excellent agreement with the 61-meV difference predicted by the separate calculations (binding energies of 24 and 85 meV [3,4]). A small shift in the diagonal elements of the $4f^2$ configuration block moves this level into the position determined by the segregated $4f^3$ and $4f^2$ calculations prior to the transition probability calculations.

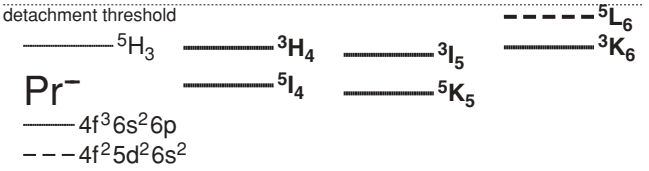

FIG. 3. Bound states of Pr^- with J increasing to the right; the predicted electron affinity is 0.177 eV [3], and the $^5L_6$ level of interest can decay by $M1$ or $E2$ emission to any of the other states in bold.

TABLE VI. Lifetimes and decay branches of bound excited states of Pr^-. The $4f^25d^26s^2\ ^5L_6$ level is a $6s$ attachment to an excited neutral threshold, while the rest are $6p$ attachments to the $4f^36s^2$ Pr ground state. Energy differences (meV) are from the most recent lanthanide RCI electron-affinity studies [3,4], and the exponents in the Einstein A coefficients (s^{-1}) are abbreviated; i.e., $1.2[-3] \equiv 1.2 \times 10^{-3}$. The bold entries represent the $^5L_6$ level of interest and its five possible decay channels.

Level (τ) Branch (ΔE)	Einstein A coefficient	
	$M1$	$E2$
$^5H_3$ 21 m		
$\rightarrow\ ^5I_4$ 79	7.7[−4]	2.0[−6]
$\rightarrow\ ^3H_4$ 4	1.1[−8]	8.3[−16]
$\rightarrow\ ^5K_5$ 95		1.8[−5]
$\rightarrow\ ^3I_5$ 18		1.2[−9]
$^5I_4$ 16 d		
$\rightarrow\ ^5K_5$ 16	7.2[−7]	2.3[−10]
$^3H_4$ 9.2 m		
$\rightarrow\ ^5I_4$ 75	1.3[−3]	2.6[−6]
$\rightarrow\ ^5K_5$ 91	4.8[−4]	1.5[−5]
$\rightarrow\ ^3I_5$ 14	1.9[−5]	1.0[−12]
$^3I_5$ 6.9 m		
$\rightarrow\ ^5I_4$ 61	1.4[−3]	1.9[−6]
$\rightarrow\ ^5K_5$ 77	1.0[−3]	5.9[−6]
$^3K_6$ 2.3 m		
$\rightarrow\ ^5I_4$ 76		5.7[−6]
$\rightarrow\ ^3H_4$ 1		2.5[−15]
$\rightarrow\ ^5K_5$ 92	7.0[−3]	6.9[−6]
$\rightarrow\ ^3I_5$ 15	2.1[−5]	1.8[−9]
$^5L_6$ 14 m		
$\rightarrow\ ^5I_4$ 137		**1.4[−8]**
$\rightarrow\ ^3H_4$ 62		**3.9[−9]**
$\rightarrow\ ^5K_5$ 153	**1.2[−3]**	**3.1[−7]**
$\rightarrow\ ^3I_5$ 76	**2.2[−6]**	**5.2[−9]**
$\rightarrow\ ^3K_6$ 61	**5.3[−6]**	**1.3[−10]**

The critical factor in the lifetime of this state as presented in Table VI is actually the small amount of mixing of a resonance state which is principally a $6p_{1/2}$ attachment to the neutral Pr $J = 11/2$ first excited state (unbound by 10 meV, the right full-square symbol in the Pr plot of Fig. 1 of our earlier RCI lanthanide study [3]). Correlation energy analysis of the two bound $J = 6$ Pr^- levels shows very small amounts of mixing between $4f^3$ and $4f^2$ configurations (only ∼25 meV compared to ∼1 eV correlation from configurations with the same $4f$ occupancy). An exception to this rule occurs if the final shift in the $4f^2$ block is adjusted to intentionally place the ^5L level within ∼10 meV of the aforementioned resonance rather than the 34- meV difference predicted by the segregated calculations [3,4] (a position that was not atypical in intermediate calculations as the RCI basis was being constructed). Within this range the two states mix as much as ∼8%, but with the proper separation, the $^5L_6$ level is just 1.2% $4f^36s^26p$. If this $^5K_6$ resonance state were hypothetically bound, its $M1$ decay rate to the $Pr^-\ ^5K_5$ ground state would result in a much shorter lifetime of ∼10 s, which is why a small amount of mixing in the $4f^25d^26s^2\ ^5L_6$ level results in a lifetime similar to that seen in the other excited $4f^36s^26p$ levels, rather than hours or days, as might otherwise be expected.

V. CONCLUSIONS

We hope that presenting some interesting features of our predicted [3–5] bound excited lanthanide and actinide anion states will encourage further experimental interest in these systems. The La^- case provides perhaps the best possible candidate for efficient laser cooling of an atomic anion, while the long-lived Lu^- and Lr^- cases serve as an extreme challenge to an ambitious and innovative experimenter.

More importantly, from the computational perspective, is that we have verified that our universal jls restriction technique is uniquely suited to application to the $4f$ and $5f$ electron subgroups in lanthanide and actinide calculations and would actually be of little utility in transition-metal cases. Also, for Pr^- at least, the validity of the assumption of minimal interaction between levels with different $4f/5f$ occupancies has been upheld; that is, while mixing was crucial to the lifetime calculation, the effect on energies in a binding energy calculation would not be significant. Without these two approximations, RCI calculations near the center of the lanthanide and actinide rows would have been too complex to attempt [3–5].

ACKNOWLEDGMENTS

Support for this work has been provided by the National Science Foundation, Grant No. PHY-0652844. Thanks also to A. Kellerbauer for useful comments regarding laser cooling of Os^-.

[1] R. C. Bilodeau and H. K. Haugen, Phys. Rev. Lett. **85**, 534 (2000).
[2] U. Warring, M. Amoretti, C. Canali, A. Fischer, R. Heyne, J. O. Meier, Ch. Morhard, and A. Kellerbauer, Phys. Rev. Lett. **102**, 043001 (2009).
[3] S. M. O'Malley and D. R. Beck, Phys. Rev. A **78**, 012510 (2008).
[4] S. M. O'Malley and D. R. Beck, Phys. Rev. A **79**, 012511 (2009).
[5] S. M. O'Malley and D. R. Beck, Phys. Rev. A **80**, 032514 (2009).
[6] S. H. Vosko, J. B. Lagowski, I. L. Mayer, and J. A. Chevary, Phys. Rev. A **43**, 6389 (1991).
[7] X. Cao and M. Dolg, Phys. Rev. A **69**, 042508 (2004).
[8] A. M. Covington, D. Calabrese, J. S. Thompson, and T. J. Kvale, J. Phys. B **31**, L855 (1998).
[9] V. T. Davis and J. S. Thompson, Phys. Rev. Lett. **88**, 073003 (2002).

[10] S. M. O'Malley and D. R. Beck, Phys. Rev. A **61**, 034501 (2000).
[11] A. Kellerbauer and J. Walz, New J. Phys. **8**, 45 (2006).
[12] A. Fischer, C. Canali, U. Warring, and A. Kellerbauer, Phys. Rev. Lett. **104**, 073004 (2010).
[13] P. L. Norquist and D. R. Beck, Phys. Rev. A **61**, 014501 (1999).
[14] D. R. Beck and E. Domeier, Can. J. Phys. **87**, 75 (2009).
[15] E. Eliav, U. Kaldor, and Y. Ishikawa, Phys. Rev. A **52**, 291 (1995).
[16] A. Borschevsky, E. Eliav, M. J. Vilkas, Y. Ishikawa, and U. Kaldor, Eur. Phys. J. D **45**, 115 (2007).
[17] S. Fritzsche, C. Z. Dong, F. Koike, and A. Uvarov, Eur. Phys. J. D **45**, 107 (2007).
[18] Y. Zou and C. F. Fischer, Phys. Rev. Lett. **88**, 183001 (2002).
[19] S. M. O'Malley and D. R. Beck, Phys. Rev. A **77**, 012505 (2008).